IMAGE ORIENTATION AND OBJECT RECONSTRUCTION VIA POINTS ON COUNTOURS

Dietmar LEGENSTEIN[1]
Vienna University of Technology, Austria
Institute of Photogrammetry and Remote Sensing
dl@ipf.tuwien.ac.at

Working Group III/2

KEY WORDS: Surface reconstruction, Orientation, Mathematical models.

ABSTRACT

The main task in photogrammetry is the reconstruction of three-dimensional objects - size, shape, position or geometric distance - from analog or digital images. In a first step the camera position and the orientation parameters are calculated from known objects within the image. The widespread procedure for solving the problem of image orientation and object reconstruction uses control points or free-form features. In the present paper object reconstruction and object orientation via contours are discussed. Points on the contour are used if a limited number of control points are accessible and measurements of additional control points lead to prohibitive efforts. For object reconstruction digital photogrammetry can be used, because lines detected automatically have to be identified with contours.
In the first part of the paper the necessary mathematical and photogrammetric methods for the solution of the tasks are developed. The second part deals with the strong dependency between the goodness of the approximation for the points on the contour and the convergence.

KURZFASSUNG

Die Hauptaufgabe der Photogrammetrie ist es, aus analogen oder digitalen Bildern dreidimensionale Objekte - Größe, Form, Lage oder geometrische Abstände - zu rekonstruieren. Dazu werden zunächst aus Photos mit Hilfe von bekannten „Gebilden“ die Aufnahmeorte und die Orientierungsparameter bestimmt. In erster Linie werden Bildorientierung und Objektrekonstruktion mittels Paßpunkten - oder auch über kurvenförmige Merkmale - gelöst. In dieser Arbeit hingegen sollen die Objektorientierung und Objektrekonstruktion über Umrißlinien diskutiert werden. Die Einbeziehung von Umrißpunkten bei der Bildorientierung ist dann von Bedeutung, wenn am Objekt nur wenige Paßpunkte gemessen werden können und das Einmessen eines jeden weiteren Paßpunktes mit erheblichem Mehraufwand verbunden wäre. Für die Objektrekonstruktion bietet sich die digitale Photogrammetrie an, bei der zwar Linien automatisch detektiert werden können, die aber mit Umrissen identifiziert werden müssen.
Im ersten Teil der Arbeit wird das mathematische und photogrammetrische Gebäude, das für die Lösung dieser Aufgabe nötig ist, entwickelt; der zweite Teil beschäftigt sich mit der starken Abhängigkeit zwischen der Genauigkeit der Näherungswerte und dem Konvergenzverhalten.

1 INTRODUCTION

The main task in photogrammetry is the reconstruction of the object from analog or digital images [Kraus, 1994, c 3.4]. Applications stretch from short-range images of work-pieces or facades to images of the surface of the earth taken from space.
In any case the process of reconstructing the object from the image depends on the knowledge of the outer orientation. In the present paper points on contours are used to determine object orientation as well as surface parameters provided outer orientation. These points on contours form the boundary between the object and the background in the image.
Points on contours can be divided into two categories:
(a) the tangent plane in the point of the object is projecting (e.g. sphere)

[1] This work is partly supported by the Austrian Science Foundation (FWF) under grant P13167-MAT, PORTIME II.

(b) the tangent plane lies on an edge of the object forming the boundary of the image of the object (e.g. cube).
Case (b) has already been solved, so in the present work points of contours satisfying condition (a) are the only concern. From this property the condition of contour is derived: the vector **s** from the camera position $\mathbf{X_0}$ to the point on the contour **X** is perpendicular to the normal vector **n** of the surface Φ (Figure 1).
In general, a point on a given surface can be described by its image: the three unknown space co-ordinates can be determined using the two co-ordinates in the image together with the condition, that the point is on the surface. Therefore the three unknowns can be calculated from three equations. In the case of a point on the contour, the additional information of the condition of contour leads to an over-determined system of equations. In the case of a full control point three additional equations are given whereas in the present case only one additional condition leads to the overdetermination.

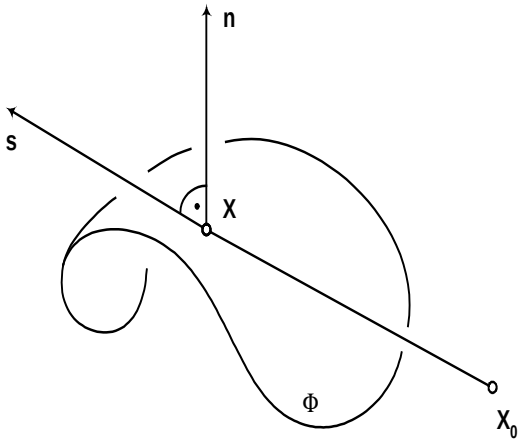

Figure 1: Condition of contour between surface, projection ray and point on contour.

2 MATHEMATICAL PRELIMINARIES

The following conventions are used for the notation of points and vectors: In general points and vectors are printed in bold letters. For algebraic treatment in calculations tensor-notation is used. If indices are used for scalar components of the elements they are printed in non-bold letters. Einstein summation convention is used for all formulas.

2.1 The Condition of Contour

A point **X** on a surface Φ is on a contour from the projection centre $\mathbf{X_0}$ if and only if the normal vector **n** of the surface Φ is perpendicular to vector **s** from the camera position to the point on the contour. This condition can be expressed with the inner product of the two vectors:

$$E_1 = n^i s_i = 0 \tag{2.1-1}$$

As mentioned above this leads to an overdetermined system of equations that can be solved using least squares approximation. Due to overdetermination discrepancies, which have to be minimised, from (2.1-1) i.e. from 0 will occur. The inner product $n^i s_i = 0$ does not allow a vivid geometric interpretation; Therefore further conditions can be used:

$$E_2 = \frac{n^i s_i}{\sqrt{n^k n_k}} = 0 \tag{2.1-2}$$

$$E_3 = \frac{n^i s_i}{\sqrt{n^k n_k}\sqrt{s^k s_k}} = 0 \tag{2.1-3}$$

In case of (2.1-2) the normal distance from the projection ray to the surface will be minimised, in case of (2.1-3) the discrepancy of the angle between **n** and **s** and a right angle will be minimised. By using one of these alternatives to (2.1-1) the user can select a suitable criterion for his application.
In photogrammetry several co-ordinate systems are used. Surfaces are often described in local co-ordinates because a suitable choice of the system can lead to a simple description. Therefore **n** is given in the model co-ordinate system (index M); on the other hand the vector **s** is determined in the image co-ordinate system (index B). For the conditions (2.1-1, 2.1-2, 2.1-3) both co-ordinate systems are transformed in a global reference system (without index). To

distinguish these indices from the tensor indices they are written in capital letters on the left-hand side of the symbols. The basic equation for the co-ordinate transformation is the spatial similarity transformation.
The transformation of the projection ray from the image co-ordinate system to the reference system is given by, where s^i is the vector in the reference system, ${}_Bs^j$ is the vector in the image system and ${}_BR^i_j$ is the rotation tensor of the similarity transformation:

$$s^i = {}_BR^i{}_j \; {}_Bs^j \tag{2.1-4}$$

The normal vector is transformed from the model co-ordinate system to the reference system. Instead of the rotation tensor ${}_BR^i_j$ the tensor ${}_MR^i_j$ of the model system has to be used, where n^i is the vector in the reference system, ${}_Mn^j$ is the vector in the model system and ${}_MR^i_j$ is the rotation tensor of the similarity transformation

$$n^i = {}_MR^i{}_j \; {}_Mn^j \tag{2.1-5}$$

The direction of the vector $\mathbf{_Bs}$ in the image system is given by the difference of the centre of projection $\mathbf{_BX_0}$ and the image co-ordinates:

$${}_Bs_i = {}_Bx_i - {}_Bx_{0i} \tag{2.1-6}$$

$$\mathbf{_BX} = \begin{pmatrix} {}_Bx_1 \\ {}_Bx_2 \\ 0 \end{pmatrix}; \quad \mathbf{_BX_0} = \begin{pmatrix} {}_Bx_{01} \\ {}_Bx_{02} \\ c \end{pmatrix}$$

${}_Bx_1$, ${}_Bx_2$	image co-ordinates of the point of contour
${}_Bx_{01}$, ${}_Bx_{02}$	principle point coordinates
c	principal distance

The direction of the surface normal vector $\mathbf{_Mn}$ in the model system, in the case of an implicitly given surface Φ is given by, where $\mathbf{_M\Phi} = \mathbf{_M\Phi}(\mathbf{_MX}) = 0$

$${}_Mn^i = \frac{\partial \, {}_M\Phi}{\partial \, {}_Mx_i} \tag{2.1-7}$$

$\mathbf{_Mn}$ is a function of $\mathbf{_MX}$ and has to be evaluated at the approximation for $\mathbf{_MX}$. In the next step the two vectors are transformed to the reference system according to (2.1-4, 2.1-5).

2.2 Linearisation of the Condition of Contour

The overdetermined system can be solved using least squares approximation [Kraus, 1994 p382ff]. Here the necessary linearisation is presented because of its importance in chapter 2.3:
Observations, e.g. image co-ordinates or conditions of contour, are functions of the unknowns:

$$l_i = f_i(x_1, x_2, x_3 \ldots x_n) \tag{2.2-1}$$

where l_i are the observations and x_i the unknowns. Observation equations like (2.2-1), cannot be used for the approximation right away because they have to be linearised beforehand. In the process of linearisation at the point ${x^0}_i$ the approximate functions l_i, that in general are non-linear, are substituted by linear ones. In the case of n unknowns this leads to an n-dimensional hyper-plane.

$$l_i = f_i(x_1, x_2, x_3 \ldots x_n) + \left(\frac{\partial f_i}{\partial x_1}\right)^0 dx_1 + \left(\frac{\partial f_i}{\partial x_2}\right)^0 dx_2 + \ldots + \left(\frac{\partial f_i}{\partial x_n}\right)^0 dx_n \qquad (2.2\text{-}2)$$

The linearisation coefficients can be combined in the tensor ${A_i}^j$:

$${A_i}^j = \left(\frac{\partial f_i}{\partial x_j}\right)^0 \qquad (2.2\text{-}3)$$

The contradictions w_i are given by the difference of the observation l_i and the evaluation of the function at the approximate values:

$$w_i = l_i - f_i\left({x_1}^0, {x_2}^0, {x_3}^0 \ldots {x_n}^0\right) \qquad (2.2\text{-}4)$$

The linearised equation can now be written as:

$${A_i}^j dx_j = w_i \qquad (2.2\text{-}5)$$

Every row of the system of equations (2.2-5) describes a differential geometric locus. In chapter 2.3 these loci are discussed in detail.
The condition of equations (2.1-1, 2.1-2) is special cases of equation (2.1-3), and therefore the linearisation coefficients of the general equation are calculated. The coefficients for the other equations can then be derived easily. In the next step the differentials for the unknown point **X** on the contour and for the surface-parameters a_i will be calculated.

Differentials for the point X on contour with coordinates x_i: Equation (2.1-3) has to be differentiated with respect to x_i. Due to the fact that the vector **s** can be written directly as the difference of the unknown point **X** on the contour and the centre of projection $\mathbf{X_0}$ in the reference system, the transformation of the image system to the reference system is not necessary.

$$s_j = x_j - x_{0j} \qquad (2.2\text{-}6)$$

Unfortunately the vector **n** cannot be written as a function of **X** right away. Therefore the transformation cannot be avoided in this case. Equations (2.1-7) and (2.1-5) have to be combined.
The differentiation of (2.1-3) with the product- and chain-rule leads to:

$$\frac{\partial E_3}{\partial x_i} = \frac{\partial E_3}{\partial n_j}\frac{\partial n_j}{\partial_M n_l}\frac{\partial_M n_l}{\partial_M x_m}\frac{\partial_M x_m}{\partial x_i} + \frac{\partial E_3}{\partial s_j}\frac{\partial s_j}{\partial x_i} \qquad (2.2\text{-}7)$$

The differential $\frac{\partial n_j}{\partial_M n_l}$ can be derived from (2.1-5) leading to:

$$\frac{\partial n_j}{\partial_M n_l} = {}_M R_j{}^l \tag{2.2-8}$$

The expression $\frac{\partial_M n_l}{\partial_M x_m}$ derived from (2.1-7) is the second derivative of the surface and therefore describes the local curvature.

$$\frac{\partial_M n_l}{\partial_M x_m} = \frac{\partial_M \Phi_{,l}}{\partial_M x_m} = {}_M \Phi_{,l}{}^m = F_l{}^m = F^m{}_l \tag{2.2-9}$$

$F^m{}_l$ is symmetric, because the order of the differential operators can be changed.

The differential $\frac{\partial_M x_m}{\partial_R x_i}$ can be calculated by inverting (2.1-5) as:

$$\frac{\partial_M x_m}{\partial_R x_i} = {}_M R^i{}_m \tag{2.2-10}$$

The differential $\frac{\partial s_j}{\partial x_i}$ according to (2.2-6) is simply the Kronecker-delta.

$$\frac{\partial s_j}{\partial x_i} = \delta_j{}^i \tag{2.2-11}$$

The calculation of $\frac{\partial E_3}{\partial n_j}$ via quotient-rule after several steps leads to:

$$\frac{\partial E_3}{\partial n_j} = \frac{1}{\sqrt{n^k n_k}\sqrt{s^k s_k}} s_n \left(\delta^{nj} - \frac{n^n n^j}{n^k n_k} \right) \tag{2.2-12}$$

A similar calculation gives the differential $\frac{\partial E_3}{\partial s_j}$:

$$\frac{\partial E_3}{\partial s_j} = \frac{1}{\sqrt{n^k n_k}\sqrt{s^k s_k}} n_l \left(\delta^{lj} - \frac{s^l s^j}{s^k s_k} \right) \tag{2.2-13}$$

Using all these parts with equation (2.2-7) leads to the differential, where further abbreviations are used:

$$\frac{\partial E_3}{\partial x_i} = \frac{1}{\sqrt{n^k n_k}\sqrt{s^k s_k}} \left(s_n \Gamma^{nj}{}_M R_j{}^l F_l{}^m{}_M R^i{}_m + n_l \Psi^{lj} \delta_j{}^i \right) \tag{2.2-14}$$

$$\Gamma^{nj} = \left(\delta^{nj} - \frac{n^n n^j}{n^k n_k} \right); \qquad \Psi^{lj} = \left(\delta^{lj} - \frac{s^l s^j}{s^k s_k} \right) \tag{2.2-15}$$

In the differentials for the variants of the condition of contour (2.1-1, 2.1-2) the tensors degenerate to the one-element, leading to the following differentials:

$$\frac{\partial E_1}{\partial x_i} = \left(s^j{}_M R_j{}^l F_l{}^m{}_M R^i{}_m + n^i \right) \tag{2.2-16}$$

$$\frac{\partial E_2}{\partial x_i} = \frac{1}{\sqrt{n^k n_k}} * \left(s_n \Gamma^{nj}{}_M R_j{}^l F_l{}^m{}_M R^i{}_m + n^i \right) \tag{2.2-17}$$

Differentials for the surface parameter a_i: According to (2.2-6) the vector **s** does not depend on the surface-parameters. Therefore the derivative of **s** with respect to a_i is zero.
The differentiation of (2.1-3) with the chain-rule leads to:

$$\frac{\partial E_3}{\partial a_i} = \frac{\partial E_3}{\partial n_j} \frac{\partial n_j}{\partial_M n_l} \frac{\partial_M n_l}{\partial a_i} \tag{2.2-18}$$

The differential $G_l{}^i = \dfrac{\partial_M n_l}{\partial a_i}$ is a double indexed tensor. Due to the strong dependency on the equation for the surface, a further calculation is pointless:

$$\frac{\partial E_3}{\partial a_i} = \frac{1}{\sqrt{n^k n_k}\sqrt{s^k s_k}} s_m \Gamma^{mj}{}_M R_j{}^l G_l{}^i \tag{2.2-19}$$

The differentials for the variants of the condition of contour (2.1-1, 2.1-2) are analogous to (2.2-16, 2.2-17):

$$\frac{\partial E_1}{\partial a_i} = s^j{}_M R_j{}^l G_l{}^i \tag{2.2-20}$$

$$\frac{\partial E_2}{\partial a_i} = s_m \Gamma^{mj}{}_M R_j{}^l G_l{}^i \tag{2.2-21}$$

The differentials with respect to the rotation tensors and the centre of projection are not quoted explicitly but can be found in [Legenstein 1997].

2.3 Rate of Convergence for the Different Conditions of Contour

The first testruns with ellipsoids have shown that the different conditions of contour lead to completely different rates of convergence. For too inaccurate approximations – greater than the radius of convergence – one of the equations leads to divergence while the others converge. The clue to the understanding of this behaviour can be found in the examination of the differential geometric loci (cf. 2.2-5). The mathematical argument can be found in the tensors Γ and Ψ. These tensors represent normal projections, orthogonal projecting a vector onto the normal planes in the direction of **n** in case of Γ, in the direction of **s** in case of Ψ. Vector fields of the normal vector of the geometric loci in the different centres of initialisation (for selected values) were plotted. If points with zero normal vectors or curls in the vector field are detected, this explains the different rate of convergence. The following images show normal vectors for differential loci. The ellipse on the left-hand side Φ represents the curve, the right one Θ the points satisfying the condition of contour. The left main vertex of the ellipse Θ is the centre of the surface, the right one the centre of projection $\mathbf{X_0}$.

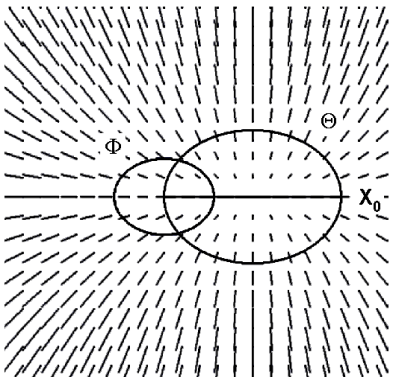

Figure 3: Normal vector field for the condition (2.1-1)

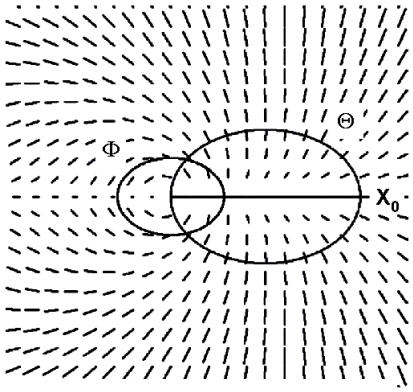

Figure 4: Normal vector field for the condition (2.1-2)

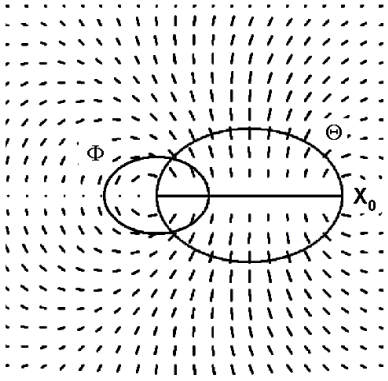

Figure 5: Normal vector field for the condition (2.1-3)

Figure 3 shows a curl-free (conservative) vector field. There is only one point with zero normal vector. This point is the middle of the centre of the surface and the centre of projection. In figure 4 a curl around the centre of the ellipsoid can be seen. In addition the normal vector is zero in this centre. This curl causes a big change in the direction of the geometric locus in these areas. This is especially disturbing because the point of contour is in that area. In figure 5 there are two curls. One of them is in the centre of the ellipsoid, the other one in the centre of projection. The normal vector is zero on the line from the centre of projection to the centre of the surface.

To determine the areas of convergence the differential loci of the contour condition are intersected with the surface condition. Both conditions have to be fulfilled for the observation of a point on contour. In addition no measurements are needed because both observations are fictitious. The intersection point is used as the next approximation value for the linearisation. In the favourable case the intersection point converges to the point of contour.

The equations for the geometric loci for the conditions of contour (2.1-1, 2.1-2, 2.1-3) can be derived from (2.2-5) in a straightforward manner using the differentials calculated above (2.2-14, 2.2-16, 2.2-17):

$$E_1: \quad \left(s^j F_j{}^i + n^i\right) dx_i = -n^k s_k \tag{2.3-1}$$

$$E_2: \quad \left(s_l \Gamma^{lj} F_j{}^i + n^i\right) dx_i = -n^k s_k \tag{2.3-2}$$

$$E_3: \quad \left(s_l \Gamma^{lj} F_j{}^i + n_l \Psi^{lj} \delta_j{}^i\right) dx_i = -n^k s_k \tag{2.3-3}$$

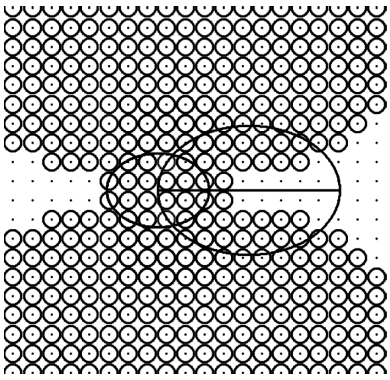

Figure 6: Area of convergence for the condition (2.1-1)

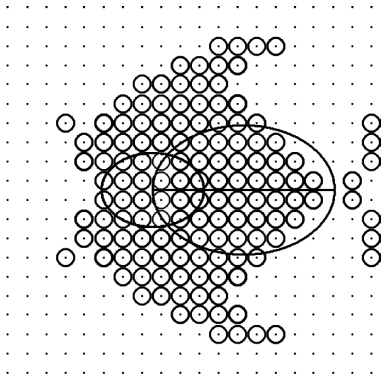

Figure 7: Area of convergence for the condition (2.1-3)

The figures 6 and 7 show the surprisingly small area of convergence for the equation (2.1-3) in contrast to the one according to (2.1-1). The circled grid points can be used as approximate values for linearisation. The figure for equation (2.1-2) was omitted because the behaviour is very similar to figure 7. Special notice should be taken of the non-connected area of convergence in the figure for the condition (2.1-3).
This method gives very precise figures for the necessary accuracy.

3 IMPLEMENTATION

For a first test of the theory the procedure was implemented in the adjustment-software ORIENT used for photogrammetric purposes. The algorithm is designed to apply the condition of contour for points on algebraic implicit surfaces up to the 9^{th} degree or to surfaces that can be described implicitly with a maximum of four parameters [Kager 2000]. In certain cases multiple iterations with one equation have to be carried out to achieve convergence with the desired condition. A suitable combination or a changing selection of one or more of the above criteria leads to the desired convergence.

4 TESTS

Testruns with numerous objects like quadrics, tori and rotation-symmetric free-form surfaces lead to the expected results: the additional over-determination lead to an increased reliability and accuracy of the desired parameters. In case of ellipsoids of revolution a special increase in the accuracy for the parameters of symmetry could be detected. Unfortunately, no results from industrial applications can be presented yet because they are just being planned for at the present time.

5 CONCLUSION AND OUTLOOK

The aim of image orientation and object reconstruction using points on contours was achieved. The theory was adapted to different representations for the surface and translated into algorithms for practical purposes. The first major application is the measurement of a pipeline-system where the advantages of a limited number of control points and the automatic detection of points on contours are especially applicable.

6 REFERENCES

[Kager, 2000] Kager, H., 2000. Adjustment of Algebraic Surfaces by Least Squared Distances, International Archives of Photogrammetry and Remote Sensing, ISPRS XIX, Amsterdam.

[Kraus, 1994] Kraus, K., 1994. Photogrammetrie, Band 1, Grundlagen und Standardverfahren, Verlag Dümmler, Bonn.

[Legenstein, 1997] Legenstein, D., 1997. Bildorientierung und Objektrekonstruktion mit Hilfe von Punkten auf Umrißlinien, Diplomarbeit, Institute of Photogrammetry and Remote Sensing.